



Two-photon superbunching effect of broadband chaotic light at the femtosecond timescale based on a cascaded Michelson interferometer

Sheng Luo ^{1,2}, Yu Zhou,¹ Huaibin Zheng ^{2,*}, Jianbin Liu,² Hui Chen,² Yuchen He,² Wanting Xu,³ Shuanghao Zhang,² Fuli Li,¹ and Zhuo Xu²

¹*MOE Key Laboratory for Nonequilibrium Synthesis and Modulation of Condensed Matter, Department of Applied Physics, Xi'an Jiaotong University, Xi'an, Shaanxi 710049, China*

²*Electronic Materials Research Laboratory, Key Laboratory of the Ministry of Education & International Center for Dielectric Research, School of Electronic Science and Engineering, Xi'an Jiaotong University, Xi'an, Shaanxi 710049, China*

³*School of Science, Xi'an Polytechnic University, Xi'an, Shaanxi 710048, China*



(Received 28 June 2020; revised 23 December 2020; accepted 4 January 2021; published 21 January 2021)

It is challenging to observe the superbunching effect with true chaotic light. Here we propose and demonstrate a method to achieve the superbunching effect of $g^{(2)}(0) = 2.42 \pm 0.02$ with broadband stationary chaotic light based on a cascaded Michelson interferometer (CMI), exceeding the theoretical upper limit of 2 for the two-photon bunching effect of chaotic light. The superbunching correlation peak is measured with an ultrafast two-photon absorption detector whose full width at half-maximum reaches about 95 fs. Two-photon superbunching theory in a CMI is developed to interpret the effect and is in agreement with experimental results. The theory also predicts that the degree of second-order coherence can be much greater than 2 if chaotic light propagates N times in a CMI. Finally, a type of weak signal detection setup that employs broadband chaotic light circulating in a CMI is proposed. Theoretically, it can increase the detection sensitivity of weak signals 79 times after the chaotic light circulates 100 times in the CMI.

DOI: [10.1103/PhysRevA.103.013723](https://doi.org/10.1103/PhysRevA.103.013723)

I. INTRODUCTION

Since Hanbury Brown and Twiss (HBT) first observed the two-photon bunching effect in 1956 [1–3], it has been well known that the degree of second-order coherence (DSOC) of thermal light equals 2 for all kinds of thermal light [4–6], including blackbody radiation [7–9], broadband amplified spontaneous emission [10–13], pseudothermal light [14–16], and so on. Although the superbunching effect of pseudothermal light has been observed [17–20], to the best of our knowledge the superbunching effect of broadband chaotic stationary light has never been measured. The reason is that one cannot artificially generate extra intensity fluctuations in a true chaotic light field as in the pseudothermal light case, and also the superbunching effect of true chaotic light itself is difficult to detect due to its femtosecond timescale coherence time.

The superbunching effect of thermal light is not only academically interesting, but it also has many important applications. In recent years, a series of studies on multiphoton effect enhancement and extreme events enhancement with bright squeezed vacuum have been reported [21,22]. The authors pointed out that these effects could be used in photon subtraction experiments [23], ghost imaging [15,24,25], and experiments that need a high multiphoton effect but low average intensity [26].

In this paper, we proposed and demonstrated a method to achieve the superbunching effect of broadband stationary chaotic light based on a cascaded Michelson interferometer (CMI). $g^{(2)}(0) = 2.42 \pm 0.02$ of stationary chaotic light is observed by using ultrafast two-photon absorption (TPA) detection technology [27,28]. This TPA detector allows us to measure the superbunching effect of chaotic stationary light at the timescale of a few femtoseconds. The superbunching effect reported in this paper is achieved without any nonlinear process involved. A theory based on two-photon interference is developed and explains the experimental results very well. The theory shows that comparing with the ordinary bunching effect in the HBT interferometer, the superbunching effect in a CMI comes from the increasing number of two-photon probability amplitudes involved. Also, the theoretical study shows that this superbunching effect can reach a much higher value as the number of cascaded processes increases, which means that the number of two-photon probability amplitudes involved increases exponentially. More importantly, the sensitivity of the CMI for small phase changes increases drastically according to our numerical simulation. Finally, we propose to use a CMI as a two-photon interferometer for weak signal detection to enhance the detection sensitivity.

The paper is organized as follows. In Sec. II, we will develop the quantum theory on the superbunching effect of chaotic light based on two-photon interference and calculate its second-order coherence function. The method to realize the superbunching effect of chaotic light is also proposed. In Sec. III, with a continuous amplified spontaneous emission (ASE) incoherent light source, a CMI, and a TPA detector, the

*huaibinzheng@mail.xjtu.edu.cn

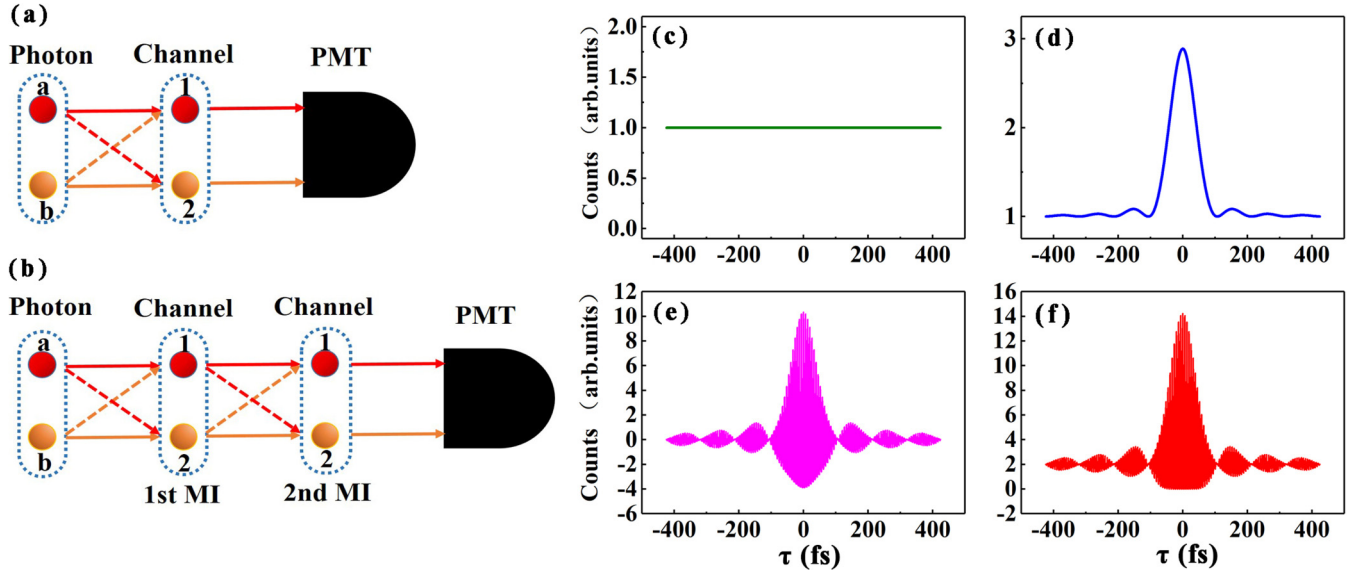


FIG. 1. Two-photon interference path diagram and the counts of simulated results of the chaotic light in MI. (a) A schematic diagram of the principle of two photons from chaotic light passing through MI once to trigger a TPA detector. (b) A schematic diagram of the principle of two photons from chaotic light passing through the MI twice to trigger a TPA detector. The solid and dashed lines represent the photon's propagation path. PMT is a TPA detector that simultaneously receives photons from different propagation paths. Part (c) shows the result of the normalization of the constant terms, corresponding to the first term in Eq. (5). Part (d) shows the superbunching effect of chaotic light, corresponding to the sum of the second, third, and fourth terms in Eq. (5). Part (e) shows the sum of the high-frequency oscillation terms, corresponding to the term $F(\tau)$ in Eq. (5). Part (f) shows the sum of all the terms in Eq. (5).

superbunching effect of chaotic stationary light is observed. The discussions about the physics of superbunching of chaotic light and its possible application are in Sec. IV.

II. THEORY

It is well known that the two-photon bunching effect can be explained by two-photon interference theory at the single-photon level [29]. The quantum theory of the bunching effect of chaotic stationary light in the Michelson interferometer is studied in Ref. [13]. The method to realize the superbunching effect of stationary chaotic light can be found by following the above studies. In the following, the quantum theory on the bunching effect in the Michelson interferometer is briefly reviewed, and the quantum explanation of the superbunching effect of stationary chaotic light in CMI is developed.

Figure 1(a) shows the schematic diagram of the bunching effect of chaotic light in a Michelson interferometer. We define a and b as two photons from the chaotic light. Channels 1 and 2 can be defined as paths that the photons reflect from the two arms of the Michelson interferometer, respectively. There are four different but indistinguishable ways for photons a and b to trigger the TPA detector, corresponding to four two-photon probability amplitudes: A_{a1b2} , A_{a2b1} , A_{a1b1} , and A_{a2b2} . The two-photon probability amplitude A_{a2b1} indicates that photon a is reflected by mirror 2 (in arm 2) and photon b is reflected by mirror 1 (in arm 1) before triggering the TPA detector together. The other probability amplitudes are defined similarly. In the language of quantum interference, the observed two-photon bunching effect of chaotic light in the Michelson interferometer [10–13] comes from the coherent interference of these four probability amplitudes. The proba-

bility of TPA detection C_{TPA} is

$$C_{\text{TPA}} = \langle |A_{a1b1} + A_{a1b2} + A_{a2b1} + A_{a2b2}|^2 \rangle. \quad (1)$$

There are four different and indistinguishable paths triggering the TPA detector. In this way, the two-photon bunching effect based on the superposition of different probability amplitudes is achieved [10,12,13].

The superbunching effect of the broadband chaotic light can be achieved by adding more different and indistinguishable interference paths to trigger the TPA detector. In our experiment, it is realized by making chaotic light pass through a CMI. As shown in the schematic diagram in Fig. 1(b), two photons from chaotic light pass through the same Michelson interferometer twice to trigger a TPA detector. There are 16 different and indistinguishable paths to trigger the TPA detector: A_{a11b11} , A_{a11b12} , A_{a11b21} , A_{a11b22} , A_{a12b11} , A_{a12b12} , A_{a12b21} , A_{a12b22} , A_{a21b11} , A_{a21b12} , A_{a21b21} , A_{a21b22} , A_{a22b11} , A_{a22b12} , A_{a22b21} , A_{a22b22} . The probability amplitude A_{a12b21} indicates that photon a propagates in arm 1 (with mirror 1) when it passes the Michelson interferometer for the first time, and then it enters the same Michelson interferometer again and propagates in arm 2 (with mirror 2). Simultaneously photon b propagates in arms 2 and 1 successively when it passes through the Michelson interferometer for the first and second time, respectively. Finally, photon a and photon b trigger the TPA detection event together. The meanings of the remaining probability amplitudes are similar.

The probability of TPA detection C_{TPA} is the result of the coherent superposition of the 16 different and indistinguishable probability amplitudes, which can be expressed

as [30,31]

$$C_{\text{TPA}} = \left\langle \left| \begin{matrix} A_{a11b11} + A_{a11b12} + A_{a11b21} + A_{a11b22} + \\ A_{a12b11} + A_{a12b12} + A_{a12b21} + A_{a12b22} + \\ A_{a21b11} + A_{a21b12} + A_{a21b21} + A_{a21b22} + \\ A_{a22b11} + A_{a22b12} + A_{a22b21} + A_{a22b22} \end{matrix} \right|^2 \right\rangle, \quad (2)$$

where $\langle \dots \rangle$ represents the ensemble average of all events. The probability amplitude can be written as

$$A_{amibnj} = e^{i\varphi_a} K_{ami} e^{i\varphi_b} K_{bnj}, \quad (3)$$

where φ_a and φ_b are the initial phase of photon a and photon b . K_{ami} and K_{bnj} represent the Feynman propagators of different photons, where $i, j, m, n = 1, 2$. The true thermal light source has a certain spectral distribution, which is different from the single frequency of the laser. In this case, the Feynman propagator from the thermal light can be expressed as [32]

$$K(r_2, t_2; r_1, t_1) = \int_{\omega_0 - \frac{1}{2}\Delta\omega}^{\omega_0 + \frac{1}{2}\Delta\omega} f(\omega) e^{-i[\omega(t_1 - t_2) - \vec{k}_{12} \cdot \vec{r}_{12}]} d\omega, \quad (4)$$

where $f(\omega)$ is the spectral distribution function of the light source that assumed the rectangular spectrum distribution. ω_0 is the center frequency and $\Delta\omega$ is the spectral bandwidth. All these parameters depend on the spectral characteristics of the light source we used. t_1 and t_2 represent the time at which the photon arrives at r_1 and r_2 , respectively, so $t_1 - t_2$ is the time difference between the photon from r_1 and r_2 . \vec{k}_{12} represents the vector of light waves where the photons are from r_1 to r_2 , and \vec{r}_{12} represents the difference between the position vectors of the photons from r_1 to r_2 .

Here we only concentrate on the temporal correlation of thermal light for simplicity. So substituting Eqs. (3) and (4) into Eq. (2), we obtain

$$C_{\text{TPA}} = 18(\Delta\omega)^2 + 18(\Delta\omega)^2 + 2(\Delta\omega)^2 \text{sinc}^2(\Delta\omega\tau) + 32(\Delta\omega)^2 \text{sinc}^2\left(\frac{1}{2}\Delta\omega\tau\right) + F(\tau). \quad (5)$$

The normalized simulation results are shown in Fig. 1, where the background of the constant term is 1. $18(\Delta\omega)^2$ is the constant term corresponding to Fig. 1(c), while $18(\Delta\omega)^2 + 2(\Delta\omega)^2 \text{sinc}^2(\Delta\omega\tau) + 32(\Delta\omega)^2 \text{sinc}^2(\frac{1}{2}\Delta\omega\tau)$ is the two-photon interference between different two-photon probability amplitudes, which leads to a background of $18(\Delta\omega)^2$ and a peak value of $34(\Delta\omega)^2$ when $\tau = 0$. This is the superbunching effect because the peak value will never surpass a background of $18(\Delta\omega)^2$ in the ordinary bunching effect. The superbunching effect in the CMI is due to the fact that the two-photon probability amplitude involved in the two-photon interference is more than those in the Michelson interferometer; the normalized function of second-order coherence is shown in Fig. 1(d). $F(\tau)$ is the high-frequency oscillation term, which is present in Fig. 1(e), where $F(\tau) = 32(\Delta\omega)^2 \cos(2\omega_0\tau) \text{sinc}^2(\frac{1}{2}\Delta\omega\tau) + 2(\Delta\omega)^2 \cos(4\omega_0\tau) \times \text{sinc}^2(\Delta\omega\tau) + 96(\Delta\omega)^2 \cos(\omega_0\tau) \text{sinc}(\frac{1}{2}\Delta\omega\tau) + 24(\Delta\omega)^2 \times \cos(2\omega_0\tau) \text{sinc}(\Delta\omega\tau) + 32(\Delta\omega)^2 \cos(\omega_0\tau) \text{sinc}(\frac{1}{2}\Delta\omega\tau) \times \cos(2\omega_0\tau) \text{sinc}(\Delta\omega\tau)$. The result of Fig. 1(f) signifies the sum of all the terms corresponding to the whole detection event C_{TPA} . The normalizing of the second-order coherence

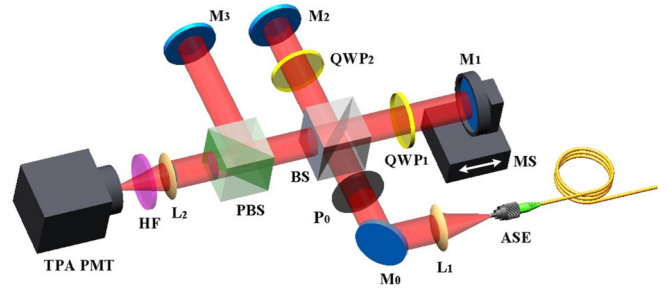


FIG. 2. Experimental setup of superbunching thermal light based on CMI. M_0 , M_1 , M_2 , and M_3 are 1550 nm dielectric mirrors, where M_1 is fixed on a precise motorized linear translation stage (MS). PMT is a GaAs photomultiplier tube.

function is given by

$$g^{(2)}(\tau) = 1 + \frac{16}{9} \text{sinc}^2\left(\frac{1}{2}\Delta\omega\tau\right) + \frac{1}{9} \text{sinc}^2(\Delta\omega\tau), \quad (6)$$

where $\text{sinc}(x) = \sin(x)/x$. When τ equals zero, $g^{(2)}(\tau) = 2.89$, which means the superbunching effect of the broadband chaotic light can be observed in the CMI scheme.

III. EXPERIMENTAL IMPLEMENTATION AND RESULTS

The method of observing the superbunching effect of chaotic stationary light is to make the chaotic light pass through a CMI. In the CMI, the two-photon interference effect is enhanced and the superbunching effect can be observed. The detailed theoretical analysis is in Sec. II, and in this section we will focus on how to realize the CMI and report the experimental results.

The experimental setup for observing the superbunching effect of broadband chaotic light is shown in Fig. 2. The light source is a continuous amplified spontaneous emission (ASE) incoherent light. Its center wavelength is 1550 nm with a bandwidth of 30 nm. L_1 and L_2 are two convergent lenses with focal lengths of 10 and 25.4 mm, respectively. P_0 is a linear polarizer with a horizontal direction. QWP_1 and QWP_2 are two quarter-wave plates with an angle of 45° between the optical axes and the polarization direction of the incident light. The broadband light is collimated by L_1 and it passes through P_0 , which causes the unpolarized chaotic light to be horizontally polarized and enter the Michelson interferometer for the first time. After passing through the nonpolarizing beamsplitter cube (BS), two split light beams pass through QWP_1 and QWP_2 , they are reflected back from M_1 and M_2 , and then they pass through QWP_1 and QWP_2 again, respectively. At that moment the polarizations of two beams changed from horizontal to vertical. Then all vertically polarized light will be reflected to M_3 by a polarizing beam-splitter cube (PBS). The light reflected by M_3 will go into the Michelson interferometer for the second time. By manipulating the polarization of light beams, we realize the function of a CMI. Finally, after the light interferes in the Michelson interferometer the second time, the vertically polarized light becomes horizontally polarized because of QWP_1 and QWP_2 . Then two horizontally polarized light beams reflected from M_1 and M_2 pass through the PBS, a spherical lens (L_2), and

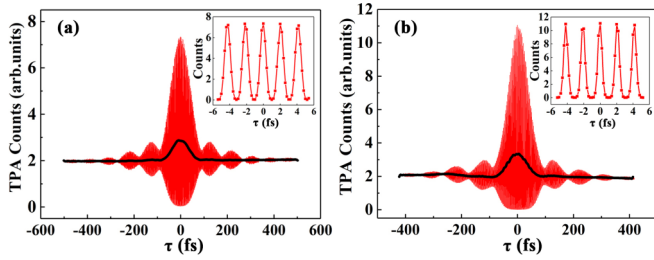


FIG. 3. (a) The measurement results of the broadband chaotic light bunching effect when light passes through the Michelson interferometer. (b) The measurement results based on the broadband chaotic light superbunching effect when light passes through the Michelson interferometer twice in succession. The red line is a graph of all counting results of the TPA detector. The black solid line is the result of filtering out high-frequency terms after numerical signal processing. The insets in (a) and (b) illustrate the enlarged detail of the interferogram near 0 fs, respectively.

a high pass filter (HF) to trigger an H7421-50 Hamamatsu GaAs-photomultiplier tube (PMT) operated in two-photon absorption mode [10]. During the experiment, the dark counts is 80 per second. The spherical lens and the high-pass filter with a cutoff wavelength of 1300 nm are used to eliminate the single-photon counting of the PMT and make sure the PMT is working in TPA mode.

To make a comparison between the ordinary bunching effect [10–12] and the superbunching effect of broadband stationary chaotic light, we first measured its photon bunching effect. This is realized by removing the PBS and M_3 from the setup shown in Fig. 2. The setup is a standard Michelson interferometer without the PBS and M_3 , and chaotic light will only circulate once before it is detected by the TPA detector. The second-order coherence function of the bunching effect is measured by scanning one arm of the interferometer-scanning M_1 on a motor stage (MS). The TPA counts are recorded versus the time delay difference between two arms. The experimental results are shown in Fig. 3(a). The red line is the measured second-order coherence function which full width at half-maximum (FWHM) is about 123 fs, and the visibility of the second-order interference pattern can reach 99.2%. The black solid line is the result of filtering out the high-frequency oscillation terms, and its peak-to-background ratio is about 1.44, which corresponds to the second-order coherence function $g^{(2)}(0) = 1.87 \pm 0.02$ obtained after normalization. The oscillating TPA counts near the maximum of the correlation peak are shown in greater detail in the inset of Fig. 3(a). From the point of view of quantum mechanics [13], the measured bunching effect comes from the interference of four two-photon probability amplitudes, as shown in Eq. (1). The results can also be explained in classical intensity fluctuation correlation theory [10]. Those studies facilitated the development of measuring the superbunching effect based on chaotic stationary light.

In the next step, the PBS and M_3 are put back into the setup to constitute the CMI as shown in Fig. 2. In this setup, chaotic light will circulate twice in the CMI before being detected by the TPA detector. In doing so, the two-photon interference paths increase and the two-photon interference effect is en-

hanced. The experiment results are shown in Fig. 3(b). The red line is the measured second-order coherence function whose FWHM is about 95 fs and the visibility of the second-order interference pattern can reach 99.8%. The black solid line is the result of removing the high-frequency oscillation term by numerical filtering, and its peak-to-background ratio is about 1.71, which corresponds to the second-order coherence function $g^{(2)}(0) = 2.42 \pm 0.03$ obtained after normalization. The oscillating TPA counts near the maximum of the correlation peak are shown in greater detail in the inset of Fig. 3(b).

Comparing the results of Fig. 3(a) and 3(b), we can see that the superbunching effect of broadband stationary chaotic light was observed in a CMI at the femtosecond timescale.

IV. DISCUSSIONS

A. N -order superbunching effect of chaotic light

Based on the above work, we know that the increasing number of times propagating through Michelson interferometer is actually adding different and indistinguishable two-photon interference paths. This is why we observed the superbunching effect of the broadband chaotic light in the CMI. When the beam passes N times through the Michelson interferometer, the whole TPA detection event can be expressed as

$$C_{\text{TPA}} = \left\langle \left| \sum_{i,j=1,2}^{4^N} A_{ai_1 i_2 \dots i_n, bj_1 j_2 \dots j_n} \right|^2 \right\rangle, \quad (7)$$

where $A_{ai_1 i_2 \dots i_n, bj_1 j_2 \dots j_n}$ is the probability amplitude of photons a and b passing through N times the arms of the Michelson interferometer, respectively, $i_1, i_2, \dots, i_n, j_1, j_2, \dots, j_n = 1, 2$.

However, the number of terms of probability amplitude would increase to as many as 4^N for the calculation of DSOC after transferring N times through Michelson interferometer. A method was proposed based on the calculation of the coefficient of the constant C_c and second-order coherence terms C_i . As the number of times passing through the Michelson interferometer is increased, there will be more and more high-frequency oscillation terms that need to be filtered out, and it will not make any contributions to the calculation of the second-order coherence function. Therefore, we only calculate the coefficients of C_c and C_i , which are straightforwardly related to the second-order coherence function.

After derivation, when the chaotic light transfers N times through the Michelson interferometer, the coefficient of constant terms C_c can be expressed in the TPA detection event as

$$C_c = \left(\sum_{n=0}^N (C_N^n)^2 \right)^2. \quad (8)$$

Similarly, the coefficient of second-order coherence terms C_i is statistically calculated as

$$C_i = \sum_{m=1}^N 2 \left(\sum_{n=0}^{N-m} C_N^n C_N^{m+n} \right)^2. \quad (9)$$

The specific derivations of C_c and C_i can be found in Appendix A and B.

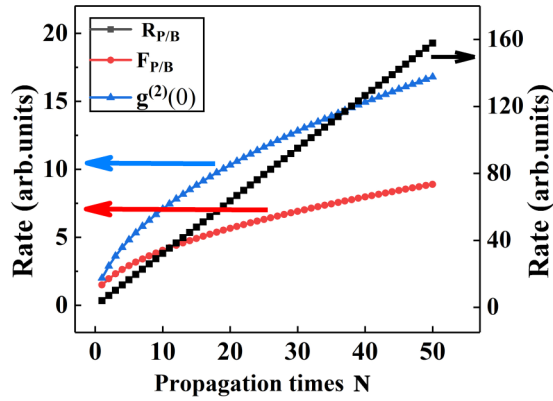


FIG. 4. Ratio of two-photon interference terms of thermal light after transferring N times through the Michelson interferometer under different conditions. The black rectangle represents $R_{P/B}$. The red circle represents $F_{P/B}$. The blue triangle represents $g^{(2)}(0)$, which is the degree of the second-order coherence of the two-photon superbunching.

To further study the N -order chaotic light superbunching effect, C_c and C_i are derived in Eqs. (8) and (9). When the beam passes through the Michelson interferometer N times, the peak-to-background ratio of the interference pattern (including high-frequency parts) of the whole TPA detection is

$$R_{P/B} = \frac{16^N}{C_c}. \quad (10)$$

Then the peak-to-background ratio of the two-photon interference pattern after filtering out the high-frequency oscillation terms is

$$F_{P/B} = 1 + \frac{C_i}{C_c}. \quad (11)$$

Naturally, the degree of the second-order coherence is

$$g^{(2)}(0) = 1 + 2\frac{C_i}{C_c}. \quad (12)$$

The numerical simulations of Eqs. (10), (11), and (12) are shown in Fig. 4, where $R_{P/B}$ increases linearly, and $F_{P/B}$ and $g^{(2)}(0)$ increase logarithmically with the increase of N . When $N = 50$, $F_{P/B} = 8.90 \pm 0.01$, $R_{P/B} = 157.87 \pm 0.02$, and $g^{(2)}(0) = 16.79 \pm 0.01$ can be obtained. Moreover, it is obvious that the increasing trend of $g^{(2)}(0)$ will gradually slow down with the increase of propagation times N . Principally as the number of times passing through the Michelson interferometer increases, the first-order interference terms inside will increase exponentially. Therefore, the increasing oscillation terms will lower the visibility and slow down DSOC growth. Nonetheless, it does not prevent us from achieving the superbunching effect of chaotic light.

B. A type of weak signals detection setup based on multiphoton interference

From the above sections, we notice that the superbunching effect in the CMI could enhance the sensitivity of phase detection. This is because multiple circulation of chaotic light in the CMI leads to multiphoton interference. Hence we propose

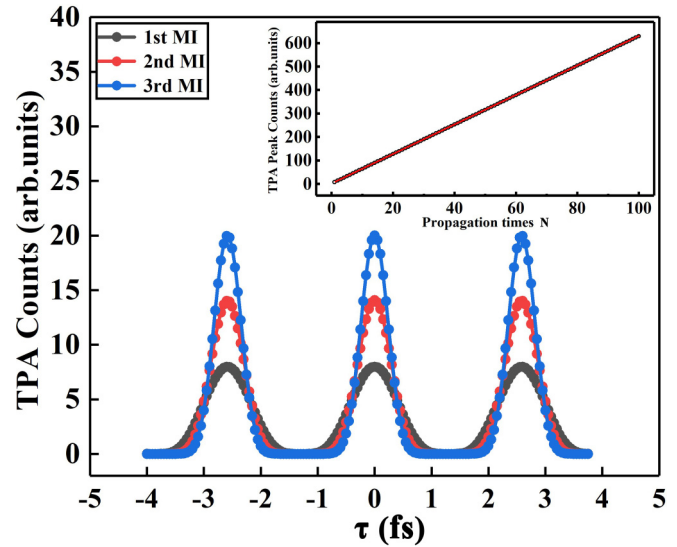


FIG. 5. The oscillatory behaviors of a TPA interferogram under different propagation times. The black, red, and blue circles represent details of the TPA detection event when chaotic light transfers through the CMI once, twice, and thrice, respectively. The inset in Fig. 5 represents the trend of the TPA peak count as propagation time increases.

to employ chaotic light circulating in the CMI to increase the sensitivity for weak signal detection. The insets in Figs. 3(a) and 3(b) illustrate the enlarged detail of the interferogram near 0 fs. It is obvious that the peak counts of chaotic light circulating twice in the CMI are higher than those circulating once in the MI (11.05 and 7.34, respectively). The numerical simulation is shown in Fig. 5 corresponding to the measurement results of the insets of Fig. 3. The black, red, and blue circles represent the details of the TPA detection event when chaotic light transferred through the CMI once, twice, and thrice, respectively. When τ equals zero, the theoretical TPA peak counts are 8, 14.22, and 20.48 separately and the period of the interference pattern is 2.55 fs. The specific theoretical derivation of chaotic light transferring through the CMI thrice is similar to Sec. II above. There are 64 different and indistinguishable two-photon interference paths that can be described by Eq. (7). Using Eq. (A3) in Appendix A and Eq. (B5) in Appendix B, the coefficients of the constant terms C_c and the second-order coherence terms C_i are 400 and 524, respectively. It is convenient to get $g^{(2)}(0) = 3.62$ from Eq. (12) when chaotic light transfers through the CMI thrice. The simulation shows that the relative TPA counts will change from 0 to 8, 14.22, and 20.48 separately when the phase changes from 0 to π . The TPA peak counts will increase with the increase of propagation times, which means the weak signal is amplified under the same phase variation.

Based on the derivation of C_c and C_i , we found that the meaning of the TPA peak counts is the same as Eq. (10) other than the different background. Therefore, the TPA peak counts can be expressed as $2R_{P/B}$. The inset in Fig. 5 illustrates that the TPA peak counts increase linearly with the increase of propagation time. When $N = 100$, the TPA peak counts equals 629.89, which means the signal amplifies 79

times compared with chaotic light circulating in the CMI once. The enhancement effect is expected to increase with the light circulating more times in the CMI. It should be emphasized that the enhancement effect is the result of multi-photon interference. As the number of times passing through the Michelson interferometer increases, the interference terms will increase exponentially. In our design, the circulation of chaotic light in the CMI provides more and more two-photon probability amplitudes interfering with each other. It not only realizes the superbunching effect of the broadband chaotic light, but it also significantly increases detection sensitivity, which provides a solution for the detection of weak signals.

V. CONCLUSIONS

In summary, the two-photon superbunching effect of broadband chaotic light is proposed and demonstrated at a femtosecond timescale based on the CMI. DSOC of chaotic light was measured as 2.42 ± 0.03 . Two-photon interference theory, which describes the superbunching effect of the broadband chaotic light in a cascade MI, has also been developed. Furthermore, we demonstrated the expression of DSOC by deriving the coefficients of the constant and second-order coherence terms when beams whose variational trends will increase with increasing N passed through a Michelson interferometer N times. Also, our numerical simulation shows that the N -order CMI dramatically improve the sensitivity of detecting small phase changes. A type of weak signal detection setup could be designed based on the superbunching effect reported in the paper. As this kind of superbunching chaotic light is simple to realize and control, it will lay a good foundation for future research on a two-photon interferometer for weak signal detection.

ACKNOWLEDGMENTS

This work was supported by Shaanxi Key Research and Development Project (Grant No. 2019ZDLGY09-09), National Natural Science Foundation of China (Grant No. 61901353), Key Innovation Team of Shaanxi Province (Grant No. 2018TD-024), and 111 Project of China (Grant No. B14040).

S.L. and Y.Z. both contributed equally to this work.

APPENDIX A: THE COEFFICIENT OF THE CONSTANT TERMS C_c OF CHAOTIC LIGHT TRANSFERRING THROUGH THE MICHELSON INTERFEROMETER N TIMES

When chaotic light transfers through a Michelson interferometer (MI) N times, there are 4^N kinds of different and indistinguishable two-photon interference paths. The whole two-photon absorption detection event can be expressed as Eqs. (7).

There will be 16^N terms after a modulus square. Any one of them can be expressed as $A_{ai_1i_2\cdots i_n, bj_1j_2\cdots j_n} A_{ap_1p_2\cdots p_n, bq_1q_2\cdots q_n}^*$, where $i_1, i_2, \dots, i_n, j_1, j_2, \dots, j_n = 1, 2, \dots, p_1, p_2, \dots, p_n, q_1, q_2, \dots, q_n = 1, 2, \dots$, $A_{ap_1p_2\cdots p_n, bq_1q_2\cdots q_n}^*$ is the complex conjugate of

$A_{ai_1i_2\cdots i_n, bj_1j_2\cdots j_n}$, and a and b represent two photons from the chaotic light, respectively. These symbols indicate whether each photon travels through channel 1 or channel 2 through the MI. For example, i_n indicates that the photon passes through channel i when it passes through MI N times.

Here we take $A_{ai_1i_2\cdots i_n, bj_1j_2\cdots j_n} A_{ap_1p_2\cdots p_n, bq_1q_2\cdots q_n}^*$ as an example. The Feynman propagator only considers the temporal correlation, and bringing the expression of the Feynman propagator into this formula, we can obtain

$$A_{ai_1i_2\cdots i_n, bj_1j_2\cdots j_n} A_{ap_1p_2\cdots p_n, bq_1q_2\cdots q_n}^* = \int_{\omega_0 - \frac{1}{2}\Delta\omega}^{\omega_0 + \frac{1}{2}\Delta\omega} f(\omega_a) e^{-i[\omega_a(i_1+i_2+\cdots+i_n-p_1-p_2\cdots-p_n)]} \times f(\omega_b) e^{-i[\omega_b(j_1+j_2+\cdots+j_n-q_1-q_2\cdots-q_n)]} d\omega_a d\omega_b, \quad (\text{A1})$$

where we define that $i_1, i_2, \dots, i_n, j_1, j_2, \dots, j_n = t_1, t_2, p_1, p_2, \dots, p_n, q_1, q_2, \dots, q_n = t_1, t_2$, and they represent the time that each photon reaches channel 1 and channel 2 when it passes through MI. To make Eq. (A1) be a constant term, it must also satisfy

$$\begin{aligned} i_1 + i_2 + \cdots + i_n - p_1 - p_2 - \cdots - p_n &= 0, \\ j_1 + j_2 + \cdots + j_n - q_1 - q_2 - \cdots - q_n &= 0. \end{aligned} \quad (\text{A2})$$

Here we can use the idea of permutation and combination to solve this equation. Taking photon a as an example, we have the following:

(i) When there is no t_1 in i_1, i_2, \dots, i_n , the number of combinations contained is C_N^0 , and at the same time all of the t_1 in p_1, p_2, \dots, p_n must be 0 to make $i_1 + i_2 + \cdots + i_n - p_1 - p_2 - \cdots - p_n = 0$ possible. Then the total number of combinations is $(C_N^0)^2$.

(ii) When there is one t_1 in i_1, i_2, \dots, i_n , the number of combinations contained is C_N^1 , and we also have to have one t_1 in p_1, p_2, \dots, p_n that is equal to C_N^1 . Then the total number of combinations is $(C_N^1)^2$.

(iii) When there are two t_1 in i_1, i_2, \dots, i_n , the number of combinations contained is C_N^2 , and at the same time there are also two t_1 in p_1, p_2, \dots, p_n . Then the total number of combinations is $(C_N^2)^2$.

(iv) By analogy, when there are N t_1 in i_1, i_2, \dots, i_n , the number of combinations included is C_N^N . In the meantime, it must also satisfy all N t_1 in p_1, p_2, \dots, p_n . Finally, the total number of combinations at this time is $(C_N^N)^2$.

Adding up all the above combination numbers, it can be expressed as

$$(C_N^0)^2 + (C_N^1)^2 + (C_N^2)^2 + \cdots + (C_N^N)^2 = \sum_{n=0}^N (C_N^n)^2. \quad (\text{A3})$$

We just discussed the case of photon a above; the case of photon b is the same and needs to satisfy $i_1 + i_2 + \cdots + i_n - p_1 - p_2 - \cdots - p_n = 0$. Therefore, we end up with the coefficient of the constant term as

$$C_c = \left(\sum_{n=0}^N (C_N^n)^2 \right). \quad (\text{A4})$$

APPENDIX B: THE COEFFICIENT OF THE SECOND-ORDER COHERENCE TERMS C_i OF CHAOTIC LIGHT TRANSFERRING THROUGH THE MICHELSON INTERFEROMETER N TIMES

What follows is the derivation of the coefficients of the second-order coherence terms. Taking the photon a as an example, through the study of the second-order coherence terms, we find that Eq. (A1) satisfies

$$i_1 + i_2 \cdots + i_n - p_1 - p_2 \cdots - p_n = k(t_1 - t_2), \quad (\text{B1})$$

where $k = -N, -(N-1), \dots, -1, 1, \dots, (N-1), N$. To simplify our derivation process, we first consider when $k \geq 1$, that is, $k = 1, \dots, (N-1), N$. This kind of calculation result is half of all the results, and the discussions are as follows:

(1) When $i_1 + i_2 \cdots + i_n - p_1 - p_2 \cdots - p_n = (t_1 - t_2)$, there are N cases in total:

(1.1) When there is one t_1 in $i_1, i_2 \cdots i_n$, the number of combinations contained is C_N^1 , and at the same time all of the t_1 in $p_1, p_2 \cdots p_n$ must be 0 to make $i_1 + i_2 \cdots + i_n - p_1 - p_2 \cdots - p_n = (t_1 - t_2)$ possible. Then the total number of combinations is $C_N^1 C_N^0$.

(1.2) When there are two t_1 in $i_1, i_2 \cdots i_n$, the number of combinations contained is C_N^2 , and we also have to have one t_1 in $p_1, p_2 \cdots p_n$ that is equal to C_N^1 . Then the total number of combinations is $C_N^2 C_N^1$.

(1.3) When there are three t_1 in $i_1, i_2 \cdots i_n$, the number of combinations contained is C_N^3 , and at the same time there are also two t_1 in $p_1, p_2 \cdots p_n$. Finally, the total number of combinations is $C_N^3 C_N^2$.

(1.4) By analogy, when there are N t_1 in $i_1, i_2 \cdots i_n$, the number of combinations included is C_N^N , and all of them must satisfy $(N-1)t_1$. Then the whole number of combinations at this time is $C_N^N C_N^{N-1}$.

In summary, the result of the addition of all the above cases just considers the case of photon a , but the photon b situation is exactly the same. Meanwhile, when we take the value of k , all the combinations can be expressed as

$$\begin{aligned} C_1 &= 2(C_N^1 C_N^0 + C_N^2 C_N^1 + C_N^3 C_N^2 + \cdots + C_N^N C_N^{N-1})^2 \\ &= 2 \left(\sum_{n=0}^{N-1} C_N^n C_N^{n+1} \right)^2. \end{aligned} \quad (\text{B2})$$

(2) When $i_1 + i_2 \cdots + i_n - p_1 - p_2 \cdots - p_n = 2(t_1 - t_2)$, there are $(N-1)$ cases in total:

(2.1) When there are two t_1 in $i_1, i_2 \cdots i_n$, the number of combinations contained is C_N^2 , and at the same time all of the t_1 in $p_1, p_2 \cdots p_n$ must be 0 to make $i_1 + i_2 \cdots + i_n - p_1 - p_2 \cdots - p_n = 2(t_1 - t_2)$ possible. Then the total number of combinations is $C_N^2 C_N^0$.

(2.2) When there are three t_1 in $i_1, i_2 \cdots i_n$, the number of combinations contained is C_N^3 , and we also have one t_1 in $p_1, p_2 \cdots p_n$ that is equal to t_1 . Then the total number of combinations is $C_N^3 C_N^1$.

(2.3) When there are four t_1 in $i_1, i_2 \cdots i_n$, the number of combinations contained is C_N^4 , and at the same time there are also two t_1 in $p_1, p_2 \cdots p_n$. Finally, the total number of combinations is $C_N^4 C_N^2$.

(2.4) By analogy, when there are N t_1 in $i_1, i_2 \cdots i_n$, the number of combinations included is C_N^N , and at the same time all must satisfy $(N-2)t_1$. Then the number of combinations is $C_N^N C_N^{N-2}$.

In this way, the result of the addition of all the above cases only considers the case of photon a , but the case of photon b is the same. Meanwhile, when we take the value of k as $k = -N, -(N-1), \dots, -1, 1, \dots, (N-1), N$, the number of combinations can be expressed as

$$\begin{aligned} C_2 &= 2(C_N^2 C_N^0 + C_N^3 C_N^1 + C_N^4 C_N^2 + \cdots + C_N^N C_N^{N-2})^2 \\ &= 2 \left(\sum_{n=0}^{N-2} C_N^n C_N^{n+2} \right)^2. \end{aligned} \quad (\text{B3})$$

(3) Similarly to the situation discussed above, we can successively express $C_1, C_2, C_3 \cdots C_N$. When $i_1 + i_2 \cdots + i_n - p_1 - p_2 \cdots - p_n = N(t_1 - t_2)$, there is only one case that has N t_1 in $i_1, i_2 \cdots i_n$, and the number of combinations included was C_N^N . At the same time, $p_1, p_2 \cdots p_n$ must meet with no t_1 . Then the number of combinations is $C_N^N C_N^0$. When we consider the case of photons b and the value range of k , the total number of combinations at this time is expressed as

$$C_N = 2(C_N^N C_N^0)^2. \quad (\text{B4})$$

To sum up, all the discussions are added up as follows:

$$C_i = C_1 + C_2 + \cdots + C_N = \sum_{m=1}^N 2 \left(\sum_{n=0}^{N-m} C_N^n C_N^{m+n} \right)^2. \quad (\text{B5})$$

[1] R. H. Brown, R. Q. Twiss *et al.*, *Nature (London)* **177**, 27 (1956).
 [2] R. H. Brown and R. Q. Twiss, *Nature (London)* **178**, 1046 (1956).
 [3] R. H. Brown and R. Q. Twiss, *Proc. R. Soc. London A* **243**, 291 (1958).
 [4] R. J. Glauber, *Phys. Rev.* **131**, 2766 (1963).
 [5] R. J. Glauber, *Phys. Rev. Lett.* **10**, 84 (1963).
 [6] R. J. Glauber, *Rev. Mod. Phys.* **78**, 1267 (2006).
 [7] R. Loudon, *The Quantum Theory of Light* (Oxford University Press, Oxford, 1973).

[8] P. K. Tan, G. H. Yeo, H. S. Poh, A. H. Chan, and C. Kurtsiefer, *Astrophys. J. Lett.* **789**, L10 (2014).
 [9] Y.-H. Zhai, X.-H. Chen, D. Zhang, and L.-A. Wu, *Phys. Rev. A* **72**, 043805 (2005).
 [10] F. Boitier, A. Godard, E. Rosencher, and C. Fabre, *Nat. Phys.* **5**, 267 (2009).
 [11] S. Hartmann, A. Molitor, and W. Elsasser, *Opt. Lett.* **40**, 5770 (2015).
 [12] A. Shevchenko, M. Roussey, A. T. Friberg, and T. Setl, *Optica* **4**, 64 (2017).

- [13] Z. Tang, B. Bai, Y. Zhou, H. Zheng, H. Chen, J. Liu, F. Li, and Z. Xu, *IEEE Photon. J.* **10**, 1 (2018).
- [14] G. Scarcelli, A. Valencia, and Y. Shih, *Europhys. Lett.* **68**, 618 (2004).
- [15] A. Valencia, G. Scarcelli, M. D'Angelo, and Y. Shih, *Phys. Rev. Lett.* **94**, 063601 (2005).
- [16] J. Xiong, D.-Z. Cao, F. Huang, H.-G. Li, X.-J. Sun, and K.-G. Wang, *Phys. Rev. Lett.* **94**, 173601 (2005).
- [17] P. Hong, J. Liu, and G. Zhang, *Phys. Rev. A* **86**, 013807 (2012).
- [18] Y. Zhou, F.-l. Li, B. Bai, H. Chen, J. Liu, Z. Xu, and H. Zheng, *Phys. Rev. A* **95**, 053809 (2017).
- [19] B. Bai, J. Liu, Y. Zhou, H. Zheng, H. Chen, S. Zhang, Y. He, F. Li, and Z. Xu, *J. Opt. Soc. Am. B* **34**, 2081 (2017).
- [20] Y. Zhou, S. Luo, Z. Tang, H. Zheng, H. Chen, J. Liu, F. li Li, and Z. Xu, *J. Opt. Soc. Am. B* **36**, 96 (2019).
- [21] T. S. Iskhakov, A. M. Perez, K. Y. Spasibko, M. V. Chekhova, and G. Leuchs, *Opt. Lett.* **37**, 1919 (2012).
- [22] P. R. Sharapova, G. Frascella, M. Riabinin, A. M. Pérez, O. V. Tikhonova, S. Lemieux, R. W. Boyd, G. Leuchs, and M. V. Chekhova, *Phys. Rev. Research* **2**, 013371 (2020).
- [23] M. Manceau, K. Y. Spasibko, G. Leuchs, R. Filip, and M. V. Chekhova, *Phys. Rev. Lett.* **123**, 123606 (2019).
- [24] T. B. Pittman, Y. H. Shih, D. V. Strekalov, and A. V. Sergienko, *Phys. Rev. A* **52**, R3429 (1995).
- [25] K. W. C. Chan, M. N. O'Sullivan, and R. W. Boyd, *Opt. Lett.* **34**, 3343 (2009).
- [26] K. Y. Spasibko, D. A. Kopylov, V. L. Krutyanskiy, T. V. Murzina, G. Leuchs, and M. V. Chekhova, *Phys. Rev. Lett.* **119**, 223603 (2017).
- [27] A. Hayat, A. Nevet, P. Ginzburg, and M. Orenstein, *Semicond. Sci. Technol.* **26**, 083001 (2011).
- [28] A. Nevet, A. Hayat, and M. Orenstein, *Opt. Lett.* **36**, 725 (2011).
- [29] U. Fano, *Am. J. Phys.* **29**, 539 (1961).
- [30] R. Feynman and A. Hibbs, *Quantum Mechanics and Path Integrals* (McGraw-Hill, New York, 1965).
- [31] R. P. Feynman, *QED: The Strange Theory of Light and Matter* (Princeton University Press, Princeton, NJ, 1985).
- [32] M. E. Peskin and D. V. Schroeder, *An Introduction To Quantum Field Theory* (CRC, Boca Raton, FL, 1995).